

Wind Energy Potential Assessment in Douala Airport, and Identification of Favorable Areas in Vicinity

C.R. Enone Ellah^{1*}, A.L.F Epée¹, J.F. Ngbara Touafio², C. Mezoue Adiang¹ and R.M. Mouangue³

1. National Higher Polytechnic School of Douala, University of Douala, Cameroon.

2. Department of Physics, Faculty of Sciences, University of Bangui, Central African Republic.

3. Group of Research in Combustion and Green Technologies, Department of Energy Engineering, University Institute of Technologie of Ngaoundere, University of Ngaoundere, Cameroon.

Received Date 27 June 2023; Revised Date 23 September 2023; Accepted Date 24 September 2023

*Corresponding author: enonecyrille@gmail.com (C.R. Enone Ellah)

Abstract

This study aims to identify a favorable area for wind energy exploitation in the Littoral region of Cameroon. The study used the data collected by the meteorological service at the Douala International Airport. A probabilistic method based on the Weibull distribution with two parameters was used to assess the potential of the studied area. Three methods were used to determine the parameters of this distribution: the maximum likelihood method, the WASP method, and the energy pattern factor method. Statistical tests showed that the energy pattern factor method is more efficient, but the WASP software provided acceptable results. The WASP software was used to generate maps of the mean wind speed and wind power density at different heights. Two specific wind turbines were considered to calculate the annual energy production. The topography of the studied area, the obstructions around the logger, and the roughness of the terrain were all taken into account when generating the maps for the different characteristics. Finally, maps at heights of 50 and 100 m were created using the extrapolation techniques. Two zones with the highest power density were identified. In one of these locations, the wind power density could reach 54 W/m² at a height of 100 m, and the annual electrical output from a specific wind turbine could reach 1 GWh. The corresponding location is located at latitude 4.0661° North and longitude 9.8796° East.

Keywords: Wind energy, Wind power density, Wind map, Available area, extrapolation, Weibull distribution, WASP.

1. Introduction

Cameroon is not an exception to the global trend toward the development of purportedly "green" energy. In fact, according to the indicators of the National Development Strategy, the rates of access to electricity and drinking water, which were 64.7% and 63.2%, respectively, in 2014 and 2016, should rise to 90% in 2030. The development of renewable energy sources other than hydroelectricity, which makes up 73.3% of the output of the major player in the electrical energy industry, is also a part of this expansion [1]. Numerous studies have previously been conducted to support the growth of Cameroon's various renewable energy sources. Although a 42 MW wind power plant project is being prepared for the West region of Cameroon, wind energy is the one that interests us because it has not yet been utilized in the nation [2]. Studies carried out all around the world using a probabilistic technique have demonstrated that it is reliable for

calculating a site's wind potential [3–5]. There are several probabilistic models that characterize the frequency of wind speed distributions using meteorological station data, according to a survey of the literature. However, one of the most used models for determining a site's or region's wind potential is the two-parameter Weibull distribution [6, 7].

Numerous authors have employed the two-parameter Weibull distribution model in their work in Cameroon. As an example, there are Kidmo *et al.* [8] with the analysis of the usage of a wind turbine for small-scale water pumping in Cameroon's North area, Kazet *et al.* [9] and their work on wind energy resource assessment in Ngaoundere locality, Pokem *et al.* [10] with their study of wind power density in Batouri in East Region or even Kenfack-Sadem *et al.* [11] who compared it to the normal and lognormal distributions. But the general observation is that

when compared to the findings of Mouangué *et al.* [12], which show that the method chosen affects the estimation of the potential, the choice of the method of calculating the model parameters is not clearly justified. Indeed, the computation of the two parameters, namely the shape factor and the scale factor, is required for the use of this Weibull model. There are several methods for performing this computation. Thirteen methods for determining these characteristics were compared by Tonsie *et al.* [13] using the wind data gathered over a 38-year period from the NASA website (from January 1982 to December 2019). The information was comprised of the ten regional capital cities of Cameroon's average daily wind speeds. The findings of the study demonstrated that, for the city of Douala, the Maximum Likelihood Method (MLM) is superior for determining the probability density function (PDF), whereas the Method of Moments (MM) is superior for determining the cumulative density function (CDF). The Energy Pattern Factor (EPF) technique, however, may be more applicable, according to a research work by Signe *et al.* [14] that used data gathered at the Douala International Airport (from September 2011 to May 2013).

However, energy production does not always take place where the data collecting logger is situated, and it is not always feasible to place wind data gathering stations throughout the whole surface of an area in order to measure the wind potential. This is where the concept of wind resource mapping comes in. Numerous authors have done studies with the goal of creating a map of the wind resource. For the Chadian cities of Ndjamena and Faya at elevations of 80 and 100 m, Tahir *et al.* [15], [16] have performed this using wind data gathered over a 5-year period utilizing the SRTM (Shuttle Radar Topography Mission) topographic data and the WAsP and Golden software tools. Ngbara *et al.* [17], [18] used the WAsP and RETScreen Expert numerical tools to create a wind resource map for the Central African Republic cities of Bouar and Bangui based on 5 and 10 years of data, respectively. Using a database of 2430 meteorological stations. With information gathered from 42 locations over 33 years, Boudia *et al.* [19] created a wind resource map in Algeria using the same techniques (1981-2014). Additionally, in Algeria, Boudia *et al.* [20] and Sidi *et al.* [21] used the numerical tool WAsP to map the wind potential in El-Bayadh and El Golea, respectively, utilizing the data gathered over 12 years and 10 years (2007 to 2016). In Cameroon, a few studies have recently been published on the mapping of wind energy

potential in the northern region. These include Kazet *et al.* [9] in Ngaoundere locality, Tsopgni *et al.* [22] for Bitchoua Highlands, Kazet and Ndjaka [23], who produced a map for the Maroua locality, and Godwe *et al.* [24], who did the same for the entire Far North region.

The objective of the current study is to determine the most advantageous for wind energy application in this area of Littoral region. This identification will be done by estimating the annual energy production (AEP) that may be created as well as the calculation of the wind potential on the chosen site in Douala at a certain height. Finding the wind power density at various heights in the researched location is the goal in this situation. For the Weibull parameters, the extrapolation techniques made use of the Justus and Mikhail's law [25]. Three techniques will be used to estimate these Weibull parameters: the MLM, the EPF method, which is the most effective for the Douala region [26], and the WAsP method. The WAsP method is one of the most widely used methods for evaluating wind potential. Statistical analyses will be used to compare these three approaches.

2. Site Location and Data Description

The Douala International Airport's meteorological department collected the wind data utilized in this study between January 1, 2020 and December 31, 2021. The logger is located at latitude 4.0044 °N and longitude 9.7313 °E, with a height of 10 m. This data is available upon request, and include the three-hourly mean wind speed and direction. To ascertain the frequency of each class, the data was processed and organized into classes. The location of the studied site is depicted in figure 1, and some details about this data are included in table 1.

Table 1. Characteristics of the used data.

Characteristic	Value	
Frequency of zero winds	0.455	
Mean speed (m/s)	1.455 ± 0.05	
Standard deviation	1.573	
Speed frequencies	Intervals (m/s)	Frequencies
	[0 ; 1[0.455
	[1 ; 2[0.065
	[2 ; 3[0.216
	[3 ; 4[0.155
	[4 ; 5[0.076
	[5 ; 6[0.021
≥ 6	0.011	

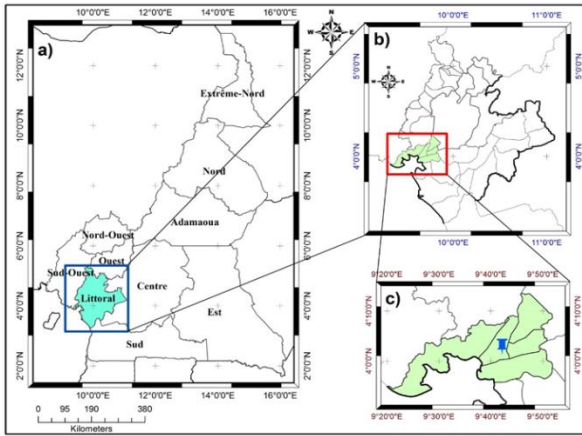


Figure 1. Location of the studied area: a) Cameroon; b) Littoral region; c) Douala.

3. Methodology

A probabilistic approach based on the two-parameter Weibull distribution was used to characterize the wind potential of the data collection point. The study of the wind atlas with WASP starts with the configuration of the topographic map from the Shuttle Radar Topography Mission data (available at <https://srtm.csi.cgiar.org/srtmdata/>). The selection of height values is based on the size-based grouping of wind turbines. Commercial wind turbines (small, medium, and large) are well-known to have rotor diameters between 10 and 100 m, which suggests that mast heights are more or less significant.

3.1. Weibull distribution

The probability density function (which represents the probability of having a given wind speed v) and the distribution function (which represents the probability of having a wind speed greater than or equal to a given speed v) are the two functions that distinguish the Weibull distribution [27]. Three methods are used here in the determination of the Weibull parameters, namely the Wind Atlas Analysis and Application Program (WASP) software suite method, the Maximum Likelihood Method (MLM), and the Energy Pattern Factor method (EPF).

• Maximum Likelihood Method (MLM)

According to MLM, the form factor and scale factor are determined from the likelihood function the expressions of k and C are given by (1) and (2), respectively.

$$k = \left(\frac{\sum_{i=1}^n v_i^k \ln v_i}{\sum_{i=1}^n \ln v_i} - \frac{\sum_{i=1}^n v_i^k}{1} \right)^{-1} \quad (1)$$

$$C = \left(\frac{1}{n} \sum_{i=1}^n v_i^k \right)^{\frac{1}{k}} \quad (2)$$

In these equations, v_i represent the measured wind speeds, and n is the total number of measurements. To find the value of k , an iterative method implemented in a C++ code was the chosen option with $k = 1$ as an initial value; the retained value is the one obtained after convergence of the solution. This value is then used to calculate C according to (2).

• Energy pattern factor method

The shape factor is calculated by (3), and the scale factor by (4) [13].

$$k = 1 + \frac{3.69}{Epf^2} \quad (3)$$

$$C = 1 + \frac{3.69}{Epf^2} \quad (4)$$

with Epf being the energy factor calculated by (5).

$$Epf = \frac{\frac{1}{n} \sum_{i=1}^n v_i^3}{\left(\frac{1}{n} \sum_{i=1}^n v_i \right)^3} \quad (5)$$

In these equations, v_i represents the measured wind speeds, n is the total number of measurements, v_m is the average speed, and $\Gamma(x)$ is the gamma function value for the variable x .

Once these methods are implemented, the accuracy of each of them is evaluated by two statistical tests: the root mean square error test (RMSE) and the coefficient of determination test (R^2). The coefficient of determination characterizes the linear relationship between the frequency values calculated by the hybrid Weibull model and the measured data. A value of R^2 close to 1 indicates the accuracy of the results of the model. The RMSE informs about the difference between the values of the frequencies of the measured speeds and those calculated by the model. A low value of the RMSE is sought for a good estimate [11], [13].

The wind power density can be obtained using (6) [28].

$$WPD = \frac{1}{2} \rho C^3 \Gamma \left(1 + \frac{3}{k} \right) \quad (6)$$

In (6), $\Gamma(x)$ is the value of the gamma function for the variable x and ρ is the air density of the site under consideration in kg/m^3 . The value used for air density in this work is the default value,

which is 1.225 kg/m^3 at the height of measurement. The vertical variation of this value is determined by logarithmic interpolation according to the relation [29]:

$$\rho = \rho_{\text{ref}} - 1.194 \times 10^{-4} \times H \quad (7)$$

where ρ is the desired density at altitude H , and ρ_{ref} is known density value for reference altitude. To calculate the AEP, specifics wind turbines where used. Table 2 shows the specifications of wind generators used for this study.

Table 2. Characteristics of the chosen turbines.

Height	50 m	100 m
Name	Nordex N50	Nordex N90-2500 LS
Manufacturer	Nordex Energy GmbH	Nordex Energy GmbH
Web link	http://www.nordex-online.com/en	http://www.nordex-online.com/en
Rotor diameter	50 m	90 m
Default height	50 m	100 m
Boot speed	4 m/s	3.5 m/s
Air density	1.225 kg/m^3	1.125 kg/m^3

3.2. Extrapolation of Weibull parameters

Wind energy is generally exploited at relatively high altitudes. However, the wind data used to characterize the wind potential of the site that is the subject of this study is taken at an altitude of 10 m. It is, therefore, imperative to use extrapolation models in order to estimate the wind power density available on this site at higher altitudes. There is a multitude models of vertical wind speed extrapolation, some of which are more complex to implement than others. The extrapolation of the Weibull parameters in this study is based on the Justus and Mikhail's law [25]. Thus to characterize the wind potential of a site with the Weibull model at different altitudes and knowing the parameters of the model at a given altitude (10 m in our case), we can extrapolate them as follows:

$$k_h = \frac{k_{10}}{1 - 0.0881 \ln \left(\frac{H}{H_{\text{ref}}} \right)} \quad (8)$$

$$C_h = C_{10} \left(\frac{H}{H_{\text{ref}}} \right)^{0.37 - 0.088 \ln C_{10}} \quad (9)$$

With: k_{10} and C_{10} representing, respectively, the shape factor and the scale factor at 10 m; k_h and C_h the shape factor and the scale factor at the desired height; H et H_{ref} the height to which one wishes to extrapolate and the reference height, respectively.

4. Results and Discussion

4.1. Statistical analysis

Table 3 shows the parameters obtained by WAsP, our code MLM, and the EPF method for each year and all 2 years combine, and table 4 shows the specifics characterizations of the for each method and each year. Here, the value of confidence intervals for key parameters estimates is determined for a confidence level of 95 %.

Table 3. Weibull parameters for the three methods.

Year	WAsP		MLM		EPF	
	k	C (m/s)	k	C (m/s)	k	C (m/s)
2020	1.190	1.500	1.220	1.250	1.000	1.240
2021	1.360	2.100	1.530	1.770	1.170	1.774
2020-2021	1.280	1.900	1.330	1.460	1.000	1.460

Table 2. Characterizations of measurement point.

Year	Method	Mean wind speed (m/s)	Standard deviation (m/s)	Wind power density (W/m ²)
2020	WAsP	1.414 ± 0.037	1.446	7.032 ± 0.250
	MLM	1.171 ± 0.031	1.2	3.801 ± 0.247
	EPF	1.240 ± 0.032	1.24	7.007 ± 0.249
2021	WAsP	1.923 ± 0.051	1.989	13.831 ± 0.253
	MLM	1.594 ± 0.043	1.666	6.553 ± 0.250
	EPF	1.680 ± 0.044	1.715	12.204 ± 0.251
2020-2021	WAsP	1.760 ± 0.046	1.812	11.800 ± 0.249
	MLM	1.342 ± 0.036	1.386	4.887 ± 0.244
	EPF	1.460 ± 0.037	1.46	11.437 ± 0.254

Considering all the data over two years, the MLM gives values all inferior to those of the other two methods. Especially for the power density, the value obtained is $4.887 \pm 0.244 \text{ W/m}^2$, and presents an average percentage of inferiority equal to 57.927%. The same method gave a power density of 3.416 W/m^2 in the work of Tonsie *et al.* [13]. This difference can be explained by the difference in the nature of the data used; Tonsie *et al.* used daily averages over 32 years for a point with different geographical coordinates from ours (Latitude 4.0429°N , Longitude 9.7062°E). Additionally, the power density value achieved by the WAsP approach is comparable to that of the EPF method. In light of this, the MLM is not the best way to make a decision in this case. This conclusion is similar to that of Signe *et al.* [14], whose work was carried out with data collected over 21 months at the Douala International Airport, which makes the EPF method the most efficient.

Figure 2 presents the probability density function for each predicted method, and from data and table 5 shows the results of statistical tests.

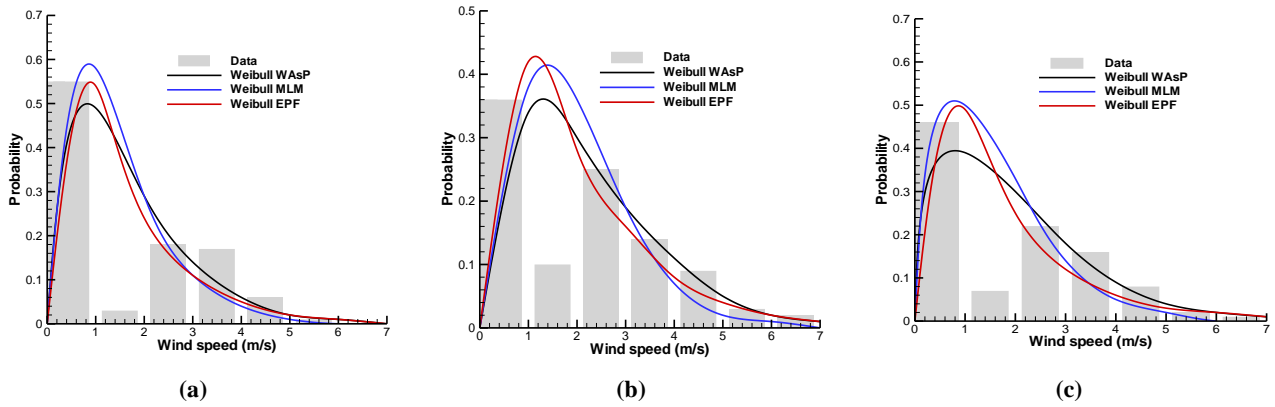


Figure 2. Weibull PDF for 2020 (a), 2021 (b), and 2020-2021 (c).

Table 3. Results of statistical tests on Weibull PDF.

Year	Method	RSME	R ²
2020	WAsP	0.111	0.835
	MLM	0.116	0.868
	EPF	0.097	0.929
2021	WAsP	0.083	0.878
	MLM	0.109	0.801
	EPF	0.086	0.949
2020-2021	WAsP	0.098	0.876
	MLM	0.114	0.901
	EPF	0.087	0.914

For the test of the coefficient of determination, a value greater than 0.9 indicates that the model fits the data very well, while a value between 0.7 and 0.9 indicates that the model fits the data well. As for the RMSE test, a value below 0.1 indicates that the model is very accurate. This being the case, the results of our statistical tests show that when there take in single years, EPF is more efficient for 2020 and WAsP is more efficient for 2021. The EPF method has a better efficiency in determining the probability density for the two years' data with a score of 0.914 according to the coefficient of determination and 0.087 according to the RMSE test.

It is possible to plot the daily and monthly wind speed profiles on, as shown in figure 3.

The daily wind speed profile shows that the winds are relatively calm (less than 2 m/s) between 9 pm and 9 am. Wind speeds become more significant between 9 am and 6 pm with a peak at 4 pm. These results are in line with the work of Mezoue *et al.* [30]. The monthly profile shows that the average monthly speeds are higher in February and from July to September. This period, which corresponds to a better energy productivity, is different from that observed in the work carried out in the north of the country by Kidmo *et al.* [31]. This difference can be explained by the nature of the climate in the two regions.

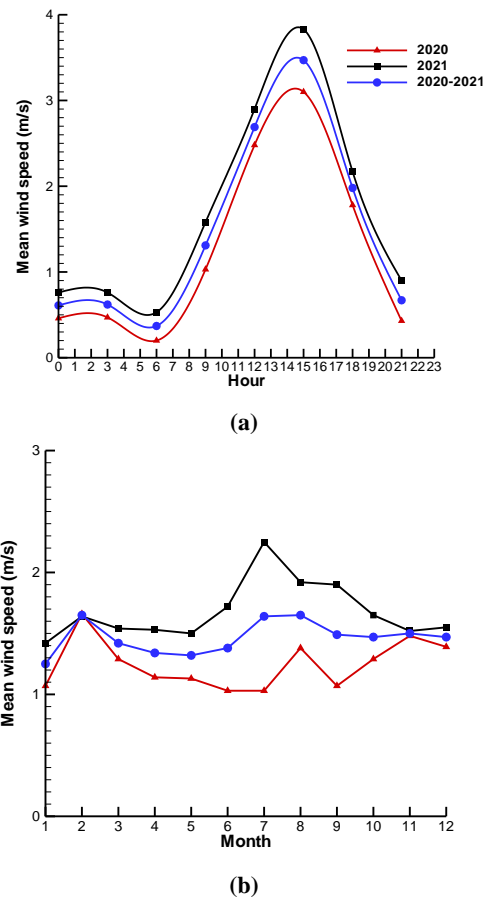


Figure 2. Daily (a) and monthly (b) wind speed profiles.

Figure 4 shows the wind rose and the Weibull probability density function for the dominant wind direction.

The preferred wind direction is southwest as in the work presented by Mezoue *et al.* [30]. In this direction, the wind moves at an average speed of 2.69 m/s and offers a wind power density equivalent to 22 W/m².

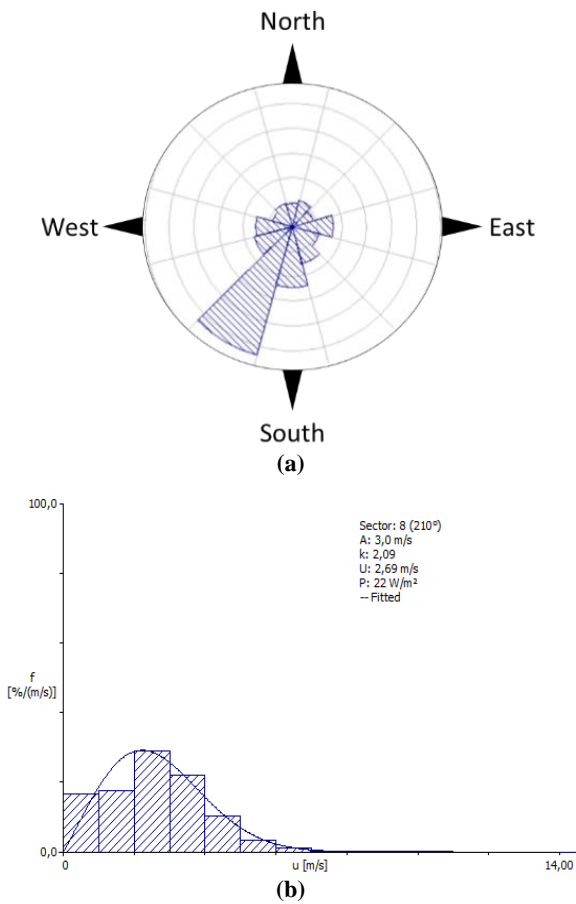


Figure 3. Wind rose and Weibull PDF for the dominant wind direction (WASP method).

4.2. Wind potential in vicinity of data collection point

Figure 5 shows the topographic map of the studied area. It shows the different elevations on the site.

The studied area's highest point, which is coloured blue, is 90 m above the sea level. Additionally, the sites in the zone taken into consideration for this study are either located worldwide at an altitude of 10 m or between 20 and 40 m.

The modelling of the barriers surrounding the mast is shown in Figure 6. The obstacle's height, depth, and porosity are all taken into account by this method. It is clear that the collecting location is in an open area.

Figure 7 is a set of maps showing different parameters at the site at the reference height (10 m). These include Weibull parameters, mean wind speed, and wind power density.

Figures 7a and 7b, respectively, allow us to observe that, in general, the studied area is covered by a form factor between 1.28 and 1.31 and a scale factor between 1.9 and 2.1 m/s. In a similar way, we can deduce from figures 7c and 7d, that this area is globally covered by an average speed between 1.75 and 1.95 m/s and a wind power density ranging from 7 to 13W/m². The

minimum values obtained are 1.35 m/s for the average speed and 5 W/m² for the wind power density, while the maximum values are 2.5 m/s and 33 W/m² respectively.

Figure 8 shows the evolution of the Weibull parameters as well as the average velocity and wind power density as a function of height at the data collection point.

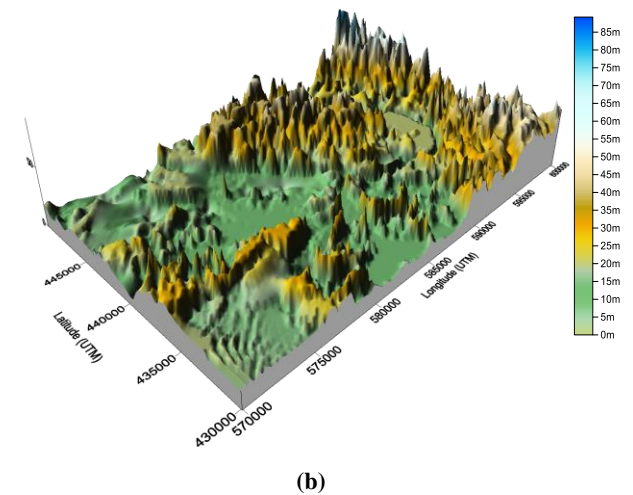
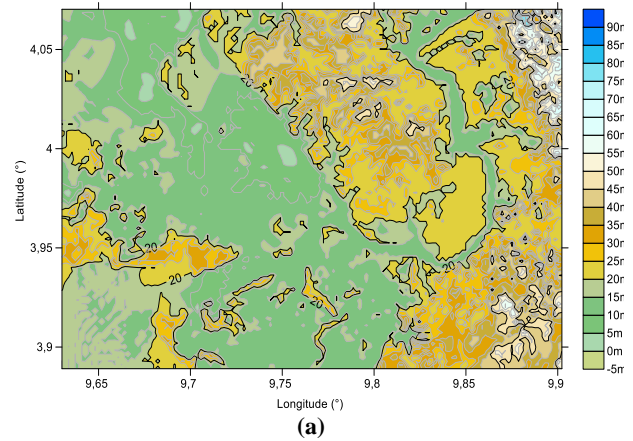


Figure 4. Representation of 2D (a) and 3D (b) numerical terrain modelling.

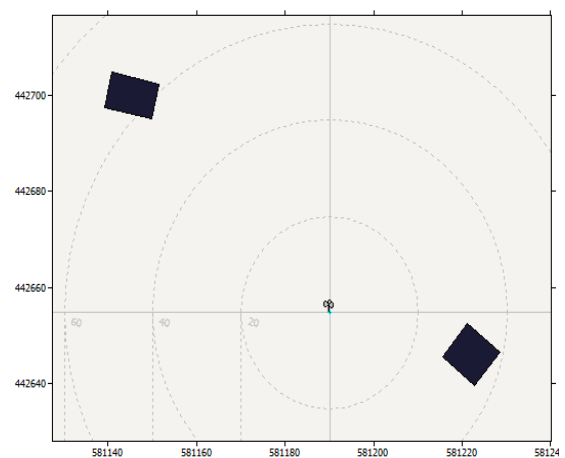


Figure 5. Modelling of obstacles around the mast.

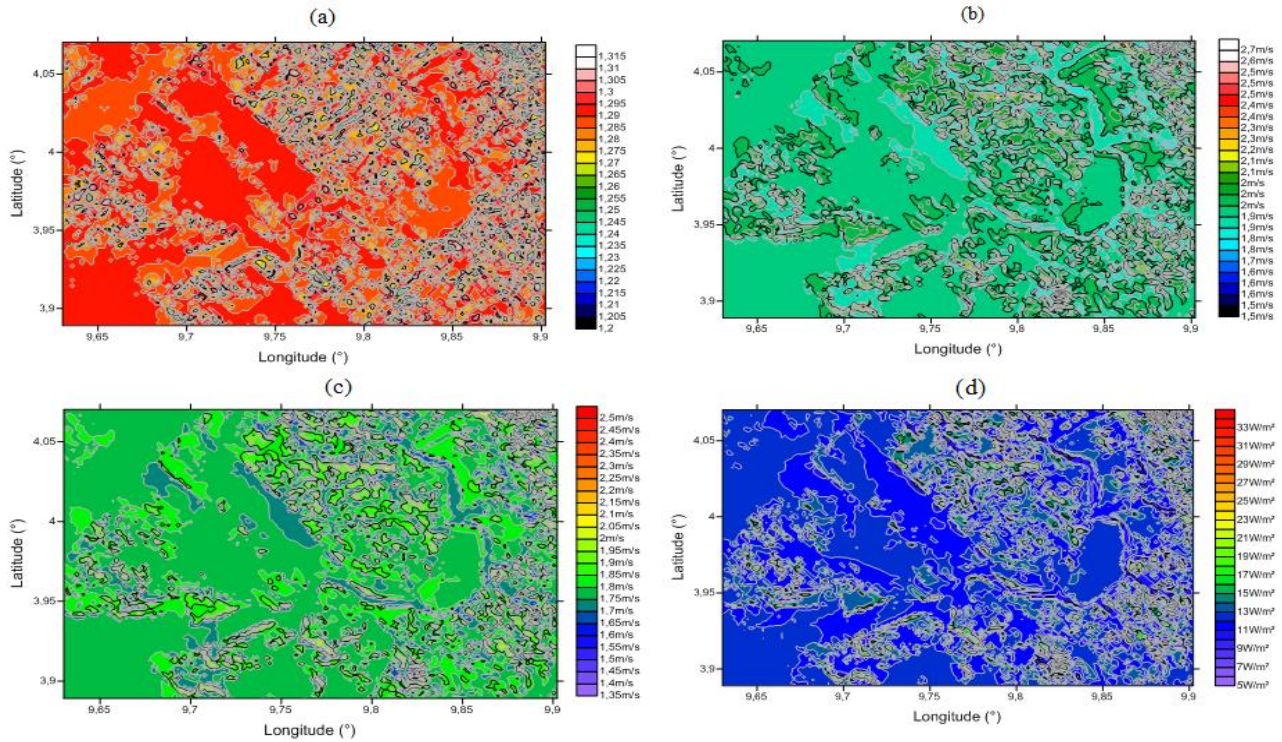


Figure 7. Maps of k (a) and C (b) parameters, mean wind speed (c), and wind power density at 10 m height.

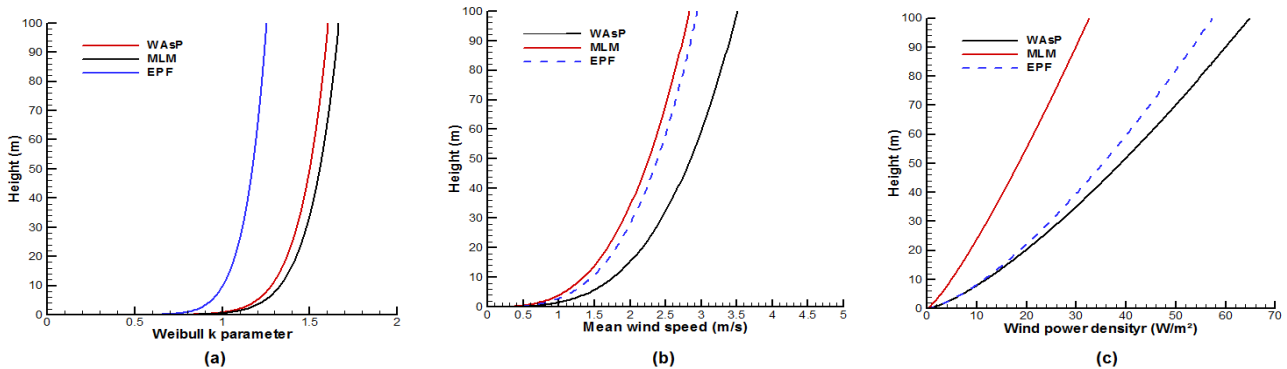


Figure 8. Extrapolation of Weibull k parameter (a), mean wind speed (b), and wind power density (c) at the measurement point.

The vertical extrapolation of the Weibull parameters shows differences in the values obtained depending on the determination method used. For the form factor, the EPF method offers values further away from the other two, while for the scale factor and the mean velocity, the WASP method is further away. If we look closely at the evolution of the power density, we are confirmed in the conclusion made above about the acceptance of the value obtained by the MLM because it is more and more far from the others. Table 6 shows the wind atlas summary containing wind parameters for 5 reference roughness lengths (0.00 m, 0.03 m, 0.10 m, 0.40 m, 1.50 m) and 3 heights (10 m, 50 m, 100 m) above ground. Figures 9 and 10 show the average wind speeds and power density extrapolated to 50 m and 100 m.

Table 6. Regional wind parameters.

Height (m)	Parameter	0.00 m	0.03 m	0.10 m	0.40 m	1.50 m
10	Weibull A (m/s)	3.5	2.5	2.1	1.7	1.2
	Weibull k	1.40	1.28	1.26	1.27	1.39
	Mean speed (m/s)	3.18	2.28	1.97	1.55	1.09
	Power density (W/m ²)	60	26	17	8	2
50	Weibull A (m/s)	4.1	3.5	3.1	2.7	2.3
	Weibull k	1.46	1.47	1.43	1.42	1.53
	Mean speed (m/s)	3.75	3.16	2.85	2.47	2.11
	Power density (W/m ²)	91	54	42	27	15
100	Weibull A (m/s)	4.5	4.2	3.8	3.3	3.0
	Weibull k	1.43	1.54	1.52	1.54	1.69
	Mean speed (m/s)	4.07	3.74	3.40	2.99	2.65
	Power density (W/m ²)	121	84	64	43	26

Legends: R-class 0: represents the surface of the water; R-class 1: the surface of the field quite little building or tree; R-class 2: territory of the land with a close appearance; R-class 3: represents a small void or territory with several broken winds; R-class 4: a big void with tall buildings.

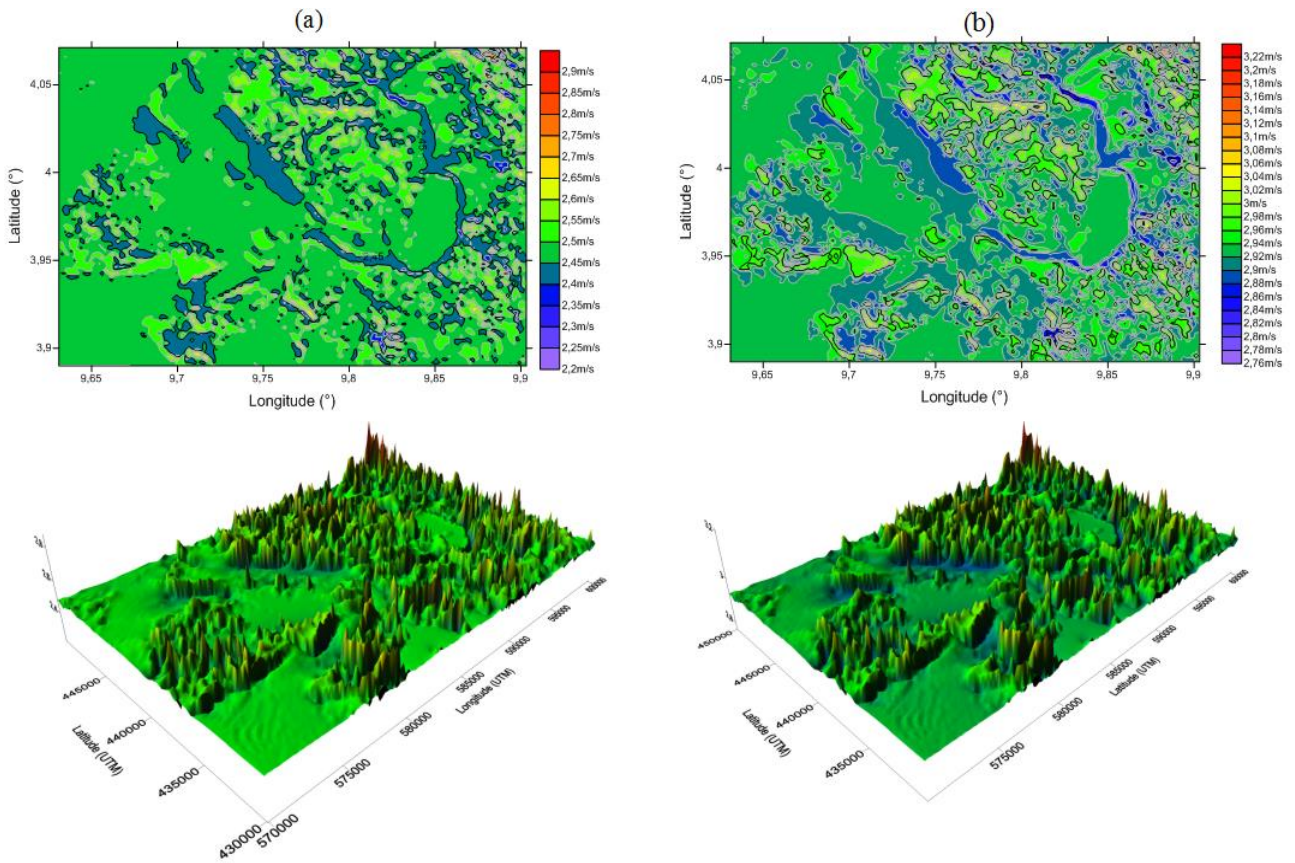


Figure 9. 2D and 3D maps of average wind speed at 50 m (a) and 100 m (b).

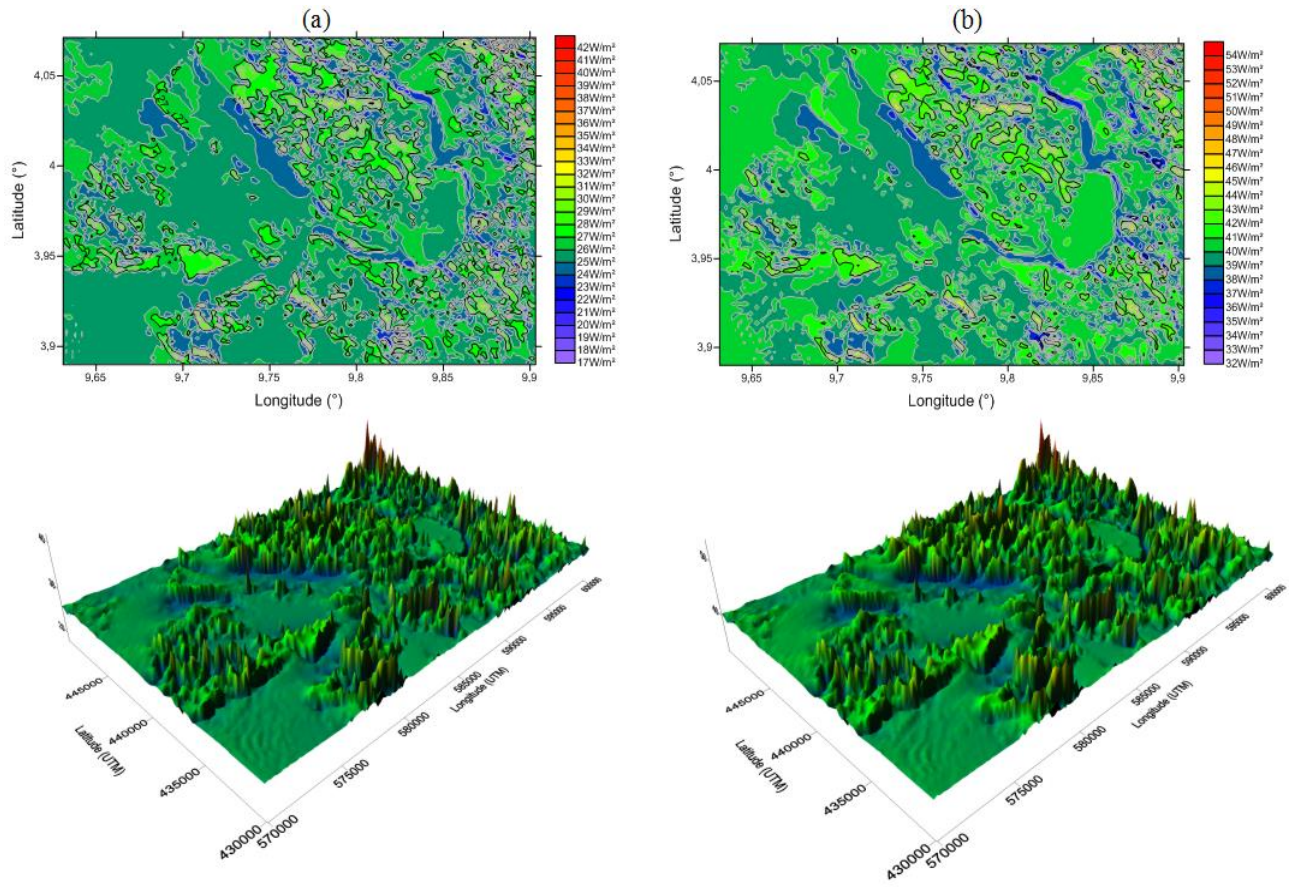


Figure 10. 2D and 3D maps wind power density at 50 m (a) and 100 m (b).

On the map of the average velocity, at a height of 50 m, it can be seen that it varies between 2.2 and 2.9 m/s, while at a height of 100 m, it is between 2.76 and 3.22 m/s. The range of average velocity values obtained at this second height is below that presented by Kazet et al. [9], which ranges from 3.25 to 4.03 m/s. One of the possible explanations for the difference is the nature of the relief of the different areas studied. In fact, the above-mentioned work was carried out for an area whose topography indicates altitudes ranging from 900 to 1500 m in the city of Ngaoundere.

From the maps of figure 10, it's possible to identify two sectors with interesting wind power densities. These sectors are presented in Figure 11. Figure 12 shows the distribution of the annual

electrical production that can be produced at 50 m to 100 m in these different sectors.

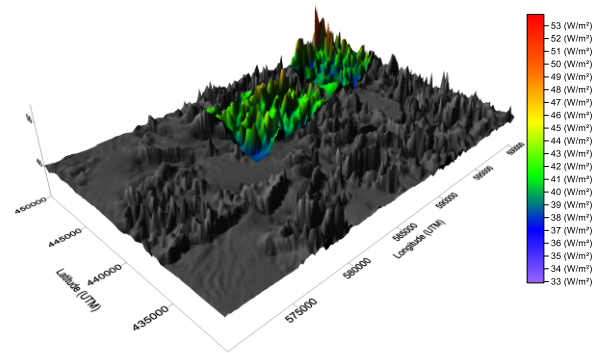


Figure 11. 3D areas with the best wind power densities for the 100 m height.

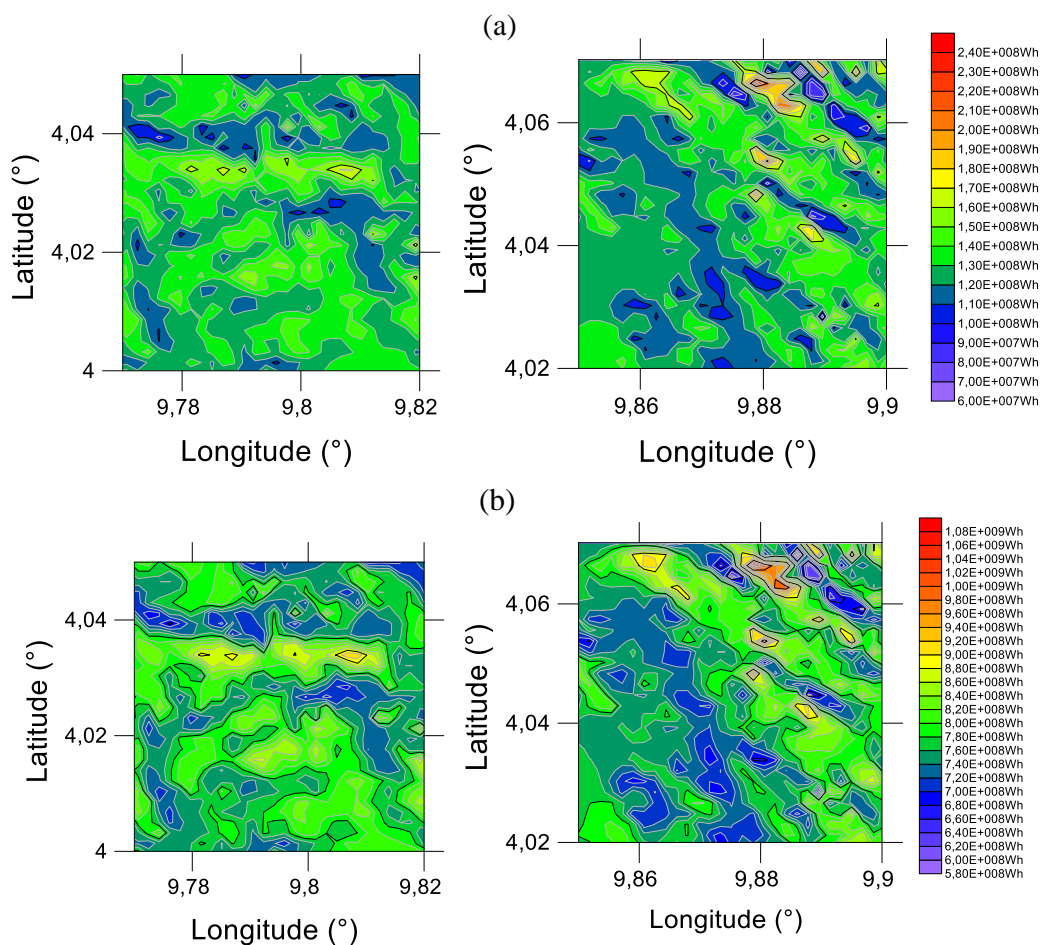


Figure 12. Annual energy production at 50 m (a) and 100 m (b) for high potential areas of the site.

The first area identified is located between the geographic coordinates (4 °N; 9.76 °E) and (4.05 °N; 9.82 °E), and covers the places called Nyalla and Japoma. The second zone is located between the points of coordinates (4.02 °N; 9.85 °E) and (4.07 °N; 9.90 °E) and passes through the village called Piti. With the wind turbine Nordex N50 considered for the height of 50 m, we have an

AEP that goes from 60 MWh, and can reach 240 MWh. When we go up to 100 m, we obtain a production that varies from 580 to 1080 MWh. The limited number of weather stations is one of the main limitations of this study, as well as those with which the mapping results are directly compared. They were all carried out on the basis of the data collected at a single measurement

point. This limitation of the wind data sources could have an influence on the accuracy of the results obtained because if other data collection points were present in the mapped area, the wind resource mapping results could be more representative of the real situation. However, the results obtained can be considered acceptable due to the fact that the studied area covers approximately 600 km².

5. Conclusion

The purpose of this study was to determine the wind potential of the Douala International Airport and its surroundings by using wind data collection single point. At the height where the data was collected, i.e. 10 m, three different methods were used to calculate the parameters of the Weibull distribution, which is the one chosen to model the wind frequencies. Statistical tests were then performed to evaluate the extent, to which the Weibull distribution predicts the probability of a certain speed. This led to the conclusion that the EPF method is the most suitable for obtaining the Weibull parameters. However, the distribution of wind frequencies shows that the site is mostly covered by zero wind with a probability of 45.5%. This is sufficient evidence that the exploitation of wind energy at this site would not be successful. However, using the WAsP and Golden Surfer software, the available wind resource around the collection point was mapped for wind exploitation. The maps created at different heights allowed us to locate two locations that can be considered as the most favorable of the site. One located between Nyalla and Japoma where the average annual wind power density can reach 47 W/m² and the annual energy produced could reach 0.9 GWh at a height of 100 m. At the same height, the other identified location which is located near the village Piti, where the average annual wind power density can reach 54 W/m² and the annual energy produced could reach 1.08 GWh.

Looking ahead, this work is in line with others that will enable a more comprehensive study to be carried out. First of all, it will be a question of extending the mapped area and associating other data collection points; this will make it possible to validate the various maps of the available energy resource. Then, once the favorable zones have been identified and inventoried, an exploration of the application to water pumping and electricity production in a parc will be carried.

6. Acknowledgments

The authors appreciatively acknowledge the chief of the weather service of the ASECNA

representation in Douala for the provision of wind data as well as the various heads of the Doctoral Training Unit of Engineering Sciences and the Doctoral School of Fundamental and Applied Sciences of the University of Douala.

7. References

- [1] ENEO, "Rapport annuel 2019," 2019. [Online]. Available: https://eneocameroun.cm/pdf/Rapport_Annuel_Eneo2019.pdf.
- [2] D. K. Kidmo, K. Deli, and B. Bogno, "Status of renewable energy in Cameroon," *Renew. Energy Environ. Sustain.*, Vol. 6, p. 2, 2021, doi: 10.1051/rees/2021001.
- [3] F. Kose, M. H. Aksoy, and M. Ozgoren, "An Assessment of Wind Energy Potential to Meet Electricity Demand and Economic Feasibility in Konya, Turkey," *Int. J. Green Energy*, Vol. 11, No. 6, pp. 559–576, 2014, doi: 10.1080/15435075.2013.773512.
- [4] S. Ersoz, T. C. Akinci, H. S. Nogay, and G. Dogan, "Determination of Wind Energy Potential in Kirklareli-Turkey," *Int. J. Green Energy*, Vol. 10, No. 1, pp. 103–116, 2013, doi: 10.1080/15435075.2011.641702.
- [5] S. Rehman and N. Natarajan, "Assessment of wind energy potential across varying topographical features of Tamil Nadu, India," *Energy Explor. Exploit.*, Vol. 38, No. 1, pp. 175–200, 2020, doi: 10.1177/0144598719875276.
- [6] D. Boro, K. Thierry, F. P. Kieno, and J. Bathiebo, "Assessing the Best Fit Probability Distribution Model for Wind Speed Data for Assessing the Best Fit Probability Distribution Model for Wind Speed Data for Different Sites of Burkina Faso," *Curr. J. Appl. Sci. Technol.*, Vol. 39, No. 22, pp. 71–83, 2020, doi: 10.9734/CJAST/2020/v39i2230845.
- [7] C. Carrillo, J. Cidrás, E. Díaz-dorado, and A. F. Obando-montaña, "An Approach to Determine the Weibull Parameters for Wind Energy Analysis: The Case of Galicia (Spain)," *energies*, pp. 2676–2700, 2014, doi: 10.3390/en7042676.
- [8] D. Kidmo Kaoga, N. Djongyang, S. Doka Yamigno, and D. Raidandi, "Assessment of wind energy potential for small scale water pumping systems in the north region of Cameroon," *Int. J. Basic Appl. Sci.*, Vol. 3, No. 1, pp. 38–46, 2014, doi: 10.14419/ijbas.v3i1.1769.
- [9] M. Y. Kazet, R. Mouangue, A. Kuitche, and J. M. Ndjaka, "Wind energy resource assessment in Ngaoundere locality," *Energy Procedia*, Vol. 93, No. March, pp. 74–81, 2016, doi: 10.1016/j.egypro.2016.07.152.
- [10] P. Pokem, E. Bertrand, K. Signe, and J. Nganhou, "Wind Speed and Power Density Analysis for Sustainable Energy in Batouri, East Region of Cameroon," pp. 44–55, 2023, doi:

10.4236/jpee.2023.116005.

[11] C. Kenfack-Sadem, R. Tagne, F. B. Pelap, and G. Nfor Bawe, "Potential of wind energy in Cameroon based on Weibull , normal , and lognormal distribution," *Int. J. Energy Environ. Eng.*, Vol. 12, No. 4, pp. 761–786, 2021, doi: 10.1007/s40095-021-00402-3.

[12] R. M. Mouangue, Y. Kazet, A. Kuitche, and J. Ndjaka, "Influence of the Determination Methods of K and C Parameters on the Ability of Weibull Distribution to Suitably Estimate Wind Potential and Electric Energy," Vol. 3, No. July, pp. 145–154, 2014, doi: 10.14710/ijred.3.2.145-154.

[13] R. H. T. Djiela, P. T. Kapen, and G. Tchuen, "Wind energy of Cameroon by determining Weibull parameters: potential of a environmentally friendly energy," *Int. J. Environ. Sci. Technol.*, No. 0123456789, 2020, doi: 10.1007/s13762-020-02962-z.

[14] E. B. Signe Kengne, A. Kanmogne, E. Guemene D, and L. Meva'a, "Comparison of seven numerical methods for determining Weibull parameters of wind for sustainable energy in Douala , Cameroon," *Int. J. Energy Sect. Manag.*, 2018, doi: 10.1108/IJESM-07-2018-0014.

[15] A. Mahamat Tahir, M. Adoum Abdraman, R. Mouangue, and A. Kuitche, "Estimate of the Wind Resource of Two Cities in the Sahara and Sahel in Chad," *Int. J. Energy Power Eng.*, Vol. 9, No. 6, p. 86, 2020, doi: 10.11648/j.ijepe.20200906.11.

[16] M. A. Abdraman, R. M. Mouangue, A. M. Tahir, and A. Kuitche, "Energy Cartography of the Wind Resource in the City of Faya and Application to Water Pumping," Vol. 4, pp. 56–67, 2019, [Online]. Available: [https://www.ias.org/ias/filedownloads/ijres/2019/020-0007\(2019\).pdf](https://www.ias.org/ias/filedownloads/ijres/2019/020-0007(2019).pdf).

[17] J. F. Ngarara, O. Sanda, S. Malenguiza, J. M. Boliguipa, and R. M. Mouangue, "Analysis of a wind turbine project in the city of Bouar (Central African Republic)," *Sci. African*, Vol. 8, No. 2020, p. e00354, doi: 10.1016/j.sciaf.2020.e00354.

[18] J. F. Ngarara, S. Malenguiza, S. Oumarou, and M. Y. Kazet, "Statistical analysis and elaboration of the wind potential map of the city of Bangui (Central African Republic)," *Reinf. Plast.*, Vol. 29, No. June, pp. 1–13, 2019, doi: 10.1016/j.ref.2019.01.001.

[19] S. M. Boudia and J. A. Santos, "Assessment of large-scale wind resource features in Algeria," *Energy*, p. 116299, 2019, doi: 10.1016/j.energy.2019.116299.

[20] S. M. Boudia, A. Yakoubi, and O. Guerri, "Wind Resource Assessment in the Western Part of Algerian Highlands, Case Study of El-Bayadh," 2018 Int. Conf. Wind Energy Appl. Alger. ICWEAA 2018, pp. 1–5, 2019, doi: 10.1109/ICWEAA.2018.8605091.

[21] S. K. Sidi and M. Boudia, "Feasibility Study of a Wind Farm in El Golea Region in the Algerian

Sahara," 2018 6th Int. Renew. Sustain. Energy Conf., pp. 1–6, doi: 10.1109/IRSEC.2018.8702902.

[22] V. Tsopgni Eneckdem, R. A. Feumba, O. Tsomo, and J. R. Bogning, "Contribution of Cartography to the Optimization of the Evaluation of Wind Energy Potential in the Republic of Cameroon: Case of Bitchoua Highlands," *J. Geogr. Environ. Earth Sci. Int.*, Vol. 25, No. 4, pp. 53–66, 2021, doi: DOI:10.9734/JGEEESI/2021/v25i430284.

[23] K. Y. Myrin and N. J. Marie, "Wind Energy Resource Assessment for Electricity Generation In Maroua," Vol. 1, pp. 38–42, 2023.

[24] V. Godwe Gormo, B. Bogno, D. Kidmo Kaoga, B. P. Ngoussandou, R. Danwe, and M. Aillerie, "Wind energy potential mapping of the far-north region of Cameroon," *AIP Conf. Proc.*, Vol. 2769, No. January, 2023, doi: 10.1063/5.0129295.

[25] M. H. Ouahabi, H. Elkhachine, F. Benabdelouahab, and A. Khamlichi, "Comparative study of five different methods of adjustment by the Weibull model to determine the most accurate method of analyzing annual variations of wind energy in Tetouan - Morocco," *Procedia Manuf.*, Vol. 46, No. 2019, pp. 698–707, 2020, doi: 10.1016/j.promfg.2020.03.099.

[26] P. Tiam Kapen, M. Jeutho Gouajio, and D. Yemélé, "Analysis and efficient comparison of ten numerical methods in estimating Weibull parameters for wind energy potential: Application to the city of Bafoussam, Cameroon," *Renew. Energy*, Vol. 159, pp. 1188–1198, 2020, doi: 10.1016/j.renene.2020.05.185.

[27] H. Mohamadi, A. Saedi, Z. Firoozi, S. Sepasi Zangabadi, and S. Veisi, "Assessment of wind energy potential and economic evaluation of four wind turbine models for the east of Iran," *Heliyon*, Vol. 7, No. 6, p. e07234, 2021, doi: 10.1016/j.heliyon.2021.e07234.

[28] P. K. Chaurasiya, S. Ahmed, and V. Warudkar, "Study of different parameters estimation methods of Weibull distribution to determine wind power density using ground based Doppler SODAR instrument," *Alexandria Eng. J.*, Vol. 57, No. 4, pp. 2299–2311, doi: 10.1016/j.aej.2017.08.008.

[29] K. S. Elie Bertrand, K. Abraham, and M. Lucien, "Sustainable Energy Through Wind Speed and Power Density Analysis in Ambam, South Region of Cameroon," *Front. Energy Res.*, Vol. 8, No. September, pp. 1–9, 2020, doi: 10.3389/fenrg.2020.00176.

[30] C. Mezoue, D. Monkam, E. Njeugna, and S. Gokhale, "Projecting impacts of two-wheelers on urban air quality of," *Transp. Res. Part D*, Vol. 52, pp. 49–63, 2017, doi: 10.1016/j.trd.2017.02.010.

[31] D. K. Kidmo, B. Bogno, K. Deli, M. Aillerie, and B. P. Ngoussandou, "Economic assessment of WECS for water pumping systems in the North Region of Cameroon," *Renew. Energy Environ. Sustain.*, Vol. 6, p. 6, 2021, doi: 10.1051/rees/2021006.